Supporting Information

In vitro, *in vivo* and spectroscopic assessment of lead exposure reduction via ingestion and inhalation pathways using phosphate and iron amendments

Farzana Kastury[1*], Euan Smith[1], Emmanuel Doelsch[1,2], Enzo Lombi[1], Martin Donnelley[3-5], Patricia L. Cmielewski[3-5], David W. Parsons[3-5], Kirk G. Scheckel[6], David Paterson[7], Martin D. de Jonge[7], Carina Herde[8], Albert L. Juhasz[1]

[1]Future Industries Institute, University of South Australia, Australia; [2]CIRAD, UPR Recyclage et risque, F-34398 Montpellier, France; [3]Women's and Children's Hospital, Adelaide, Australia; [4]Adelaide Medical School and [5]Robinson Research Institute, University of Adelaide, Australia, [6]United States Environmental Protection Agency, Cincinnati, USA; [7]Australian Synchrotron, ANSTO, Australia; [8]South Australian Health and Medical Research Institute, Adelaide, Australia

*Corresponding author: Farzana Kastury

Future Industries Institute

University of South Australia, Building X, Mawson Lakes

Campus, Adelaide, SA, 5095, Australia

Email: farzana.kastury@mymail.unisa.edu.au

Number of pages: 12

Number of Figures: 4

Number of Tables: 3

Quality assurance and quality control of soil and tissue digestion

Trace grade nitric acid was used during soil and tissue digestion and ICP analysis. The limit of detection (LOD) for Pb was 0.1 ppb with sample blanks below the LOD. Two standard reference materials (SRM) from the National Institute of Standards and Technology (NIST) were used to confirm the accuracies of digestion. The average ± SEM Pb recovery from NIST SRM 2710a (certified total 5520 ± 3 mg/kg) was 5526 ± 83.4 mg/kg ($n = 4$) and from NIST SRM 2976 (certified total 1190 ± 180 mg/kg) was 1206 ± 19.7 mg/kg ($n = 4$). During the ICP-MS analysis, Pb spiked samples and check value recoveries were included. The average deviation from check value recoveries from soil digests ($n = 10$) was 5.6%, organ digests ($n = 32$) was 5.5% and during the analysis of blood ($n = 24$) was 2.4%. The average recovery of Pb spiked samples were within the limits specified in USPEA method 6020A[1].

Application of amendments

Because the P concentrations were not known in the TSP and biochar, aqua-regia digestion was conducted to obtain P concentrations before amendment, which also showed low Pb concentration in the amendments (<40 mg/kg). To ensure that the amendments were uniform in sizes, HA, TSP and biochar were ground and sieved to < 53 μm particle size fraction prior to amendment. Amendments were added to 500 g soil at a Pb:P / Fe molar ratio of 1:5 at 80% water holding capacity. PA and MAP were dissolved in MilliQ water (>18MΩ) and stirred into the soil. Water insoluble amendments (e.g. HA, TSP, biochar, Fe_2O_3) were mixed with the soil using end-over-end rotation overnight, followed by WHC adjustment using MilliQ water.

Calculation of Pb *in vitro* bioaccessibility (IVBA)

$$Pb\ IVBA\ (\%) = \frac{In-vitro\ Pb}{Total\ pb}\ x\ 100 \ldots Eq.\ 1$$

Where:

In vitro Pb = Pb concentration (mg/L) in solution following extraction using an IVBA.

Total Pb = Pb concentration (mg/kg) in contaminated soil used in the IVBA.

Calculation of Pb relative bioavailability (RBA)

Pharmacokinetic analysis encompassing area under the PbB time curve (AUC) was utilized to assess after zero correction and dose normalization using Pb as the reference dose. Percentage Pb RBA was calculated using Eq. 2

$$Oral\ Pb\ RBA\ (\%) = \frac{AUC\ oral-soil}{AUC\ oral-Pb\ acetate} \times \frac{D\ oral-Pb\ acetate}{D\ oral-soil}\ x\ 100 \ldots\ldots.Eq.\ 2$$

Where:

AUC oral-soil = AUC following an oral Pb contaminated soil dose.

AUC oral-Pb acetate = AUC following an oral Pb acetate dose.

D oral-Pb acetate = dose of orally administered Pb acetate (mg/kg)

D oral-Pb soil = dose of orally administered Pb in contaminated soil (mg/kg)

Extended X-ray Absorption Fine Structure (EXAFS) spectroscopic assessment of Pb and Fe in phosphate amended Pb-contaminated soils and post IVBA assay residuals

EXAFS data were collected at the Materials Research Collaborative Access Team (MRCAT) beamline 10-ID at the Advanced Photon Source (APS) of the Argonne National Laboratory (ANL), U.S. The storage ring operated at 7 GeV in top-up mode. A liquid N_2 cooled double crystal Si(111) monochromator was used to select the incident photon energies and a platinum-coated mirror was used for harmonic rejection. Calibration was performed by assigning the first derivative inflection point of the absorption L_{III}-edge of Pb metal (13035 eV) or K-edge of Fe metal (7112 eV), and each sample scan was collected simultaneously with a Pb or Fe metal foil. The samples were ground and pressed into pellets, affixed to a 20-hole sample holder, and mounted for analysis without any further modifications. Data collection was conducted in fluorescence (Ge detector, Canberra) and transmission modes for the samples. For some samples, the transmission data were unusable for analysis. Various Pb standards were used as reference spectra, including mineral sorbed Pb [Pb-ferrihydrite, Pb-kaolinite, Pb-goethite, Pb-gibbsite, Pb-birnessite, and Pb-montmorillonite in which each mineral was equilibrated with $Pb(NO_3)_2$ at pH 6 for a target surface loading of 2500 mg/kg after dialysis], organic bound Pb [Pb-fulvic acid and Pb-humic acid as reagent grade organic acids equilibrated with $Pb(NO_3)_2$ at pH 6 for a target loading of 1500 mg/kg after dialysis, and reagent grade Pb acetate, Pb cysteine, and Pb citrate], Pb carbonate [Smithsonian Natural History Minerals Collection specimens of cerussite, hydrocerussite, and plumbonacrite with X-ray diffraction verification], PbO [massicot and litharge], Pb-phosphates [chloropyromorphite, hydroxypyromorphite, lead phosphate ($Pb_3(PO_4)_2$), $PbHPO_4$, and Pb sorbed to apatite at pH 6 and surface loading of 2000 mg/kg], and other lead minerals

[leadhillite, magnetoplumbite, plumboferrite, plumbogummite, plumbojarosite, anglesite, and galena from the Smithsonian Natural History Minerals Collection with X-ray diffraction verification]. Iron reference standards included ferrihydrite ($5Fe_2O_3 \cdot 9(H_2O)$), goethite (α-FeO(OH), lepidocrocite (γ-FeO(OH), maghemite (γ-Fe_2O_3), magnetite (Fe_3O_4), vivianite ($Fe_3(PO_4)_2 \cdot 8(H_2O)$), hematite ($Fe_2O_3$), pharmosiderite ($KFe_4(AsO_4)_3(OH)_4 \cdot 6$–$7(H_2O)$), and Fe-containing clays (montmorillonite, illite, and vermiculite). All reference spectra were collected in transmission mode with dilution calculations determined by XAFSMass mixed in binder and pressed into a pellet[2]. These spectra were acquired on the same beamline with identical scan parameters simultaneously with a Pb metal foil for calibration, but on separate occasions to the samples.

All sample and standard spectra were calibrated to a Pb or Fe foil on the same energy grid, averaged, and normalized, and the background was removed by spline fitting using IFEFFIT[3]. Principal components analyses were performed in Sixpack[4] on the normalized scans, and target factor analyses of each Pb or Fe standard were performed to determine the most appropriate standards to be used for linear combination fits (LCF) analyses. Pb standards with SPOIL values < 3.0 were used in the LCF analyses, which included mineral sorbed Pb [sum of Pb-ferrihydrite, Pb-goethite, and Pb-birnessite], organic bound Pb [sum of Pb-fulvic acid and Pb-humic acid], Pb carbonate [sum of cerussite and hydrocerussite], PbO [sum of massicot and litharge], Pb-phosphates [chloropyromorphite, hydroxypyromorphite, $Pb_3(PO_4)_2$, and Pb sorbed to apatite], and other lead minerals [leadhillite, plumboferrite, plumboyarosite, anglesite, and galena]. Fe LCF included goethite, ferrihydrite, magnetite, hematite, maghemite, and clay samples. The k–space functions of the standards and samples were used for all linear combination fitting. Levenberg–Marquardt least squares algorithm was applied to a fit range of 0.6 to 9.0 Å^{-1}. Best-fit scenarios, defined as having the smallest residual error, also had sums of all fractions close to 1. To fully describe any particular

sample within 1% reproducible error, a minimum of two components was necessary, and results have a ±10% accuracy.

X-ray fluorescence (XRF) microscopy images of lungs and gastrointestinal (GI) tracts and Pb speciation analysis in lungs using X-ray Absorption Near Edge Spectroscopy (XANES)

Samples were analyzed at the X-ray Fluorescence Microscopy (XFM) beamline (Australian Synchrotron, Melbourne), where an in-vacuum undulator is used to produce a brilliant X-ray beam. A Si(111) monochromator and Kirkpatrick-Baez mirrors delivered a monochromatic focused beam of ca. 2×2 µm onto the specimen[5,6]. The X-ray fluorescence emitted by the specimen was collected using the 384-element Maia detector placed in a backscatter geometry[7]. For all scans, samples were analyzed continuously in the horizontal direction ('on the fly').

Elemental mapping was conducted using an incident energy of 18.5 keV. The XANES-imaging consisted of forming 'stacks' of µ-XRF maps by scanning the entire area of interest 90 times by progressively decreasing the energy from 13.235 to 12.975 keV across the P L_{III}-edge.

All XRF spectra were analyzed using GeoPIXE and images generated using the Dynamic Analysis method[8,9]. It should be noted here that the 3 colour maps reported in Figure 3 and 4 should not be used to assess co-localisation of Pb, Fe and Ca due to the different effect that self-absorption has on the fluorescence of these 3 elements (with Ca having the lower fluorescence energy and therefore being more attenuated than the Pb signal if co-localised).

Pb XANES spectra were extracted from high and low Pb concentrations areas and normalized using Athena[3]. Pb speciation was analyzed using Linear Combination Fitting

(LCF) in a relative energy range of 13015 to 13090 eV using the smallest R-factor values to assess the best fit using the Pb standards that are depicted in Figure S1 and described in the section titled "Extended X-ray Absorption Fine Structure (EXAFS) spectroscopic assessment of Pb and Fe in phosphate amended Pb-contaminated soils and post IVBA assay residuals. For the XANES-stacks, the GeoPIXE 'energy association' module was used to identify and select areas (pixels) where the Pb concentration was high or low. For these two pixel-populations, the XANES spectra (each spectra consisting of 100 points) were extracted from the XANES-stack and the data analysed as above.
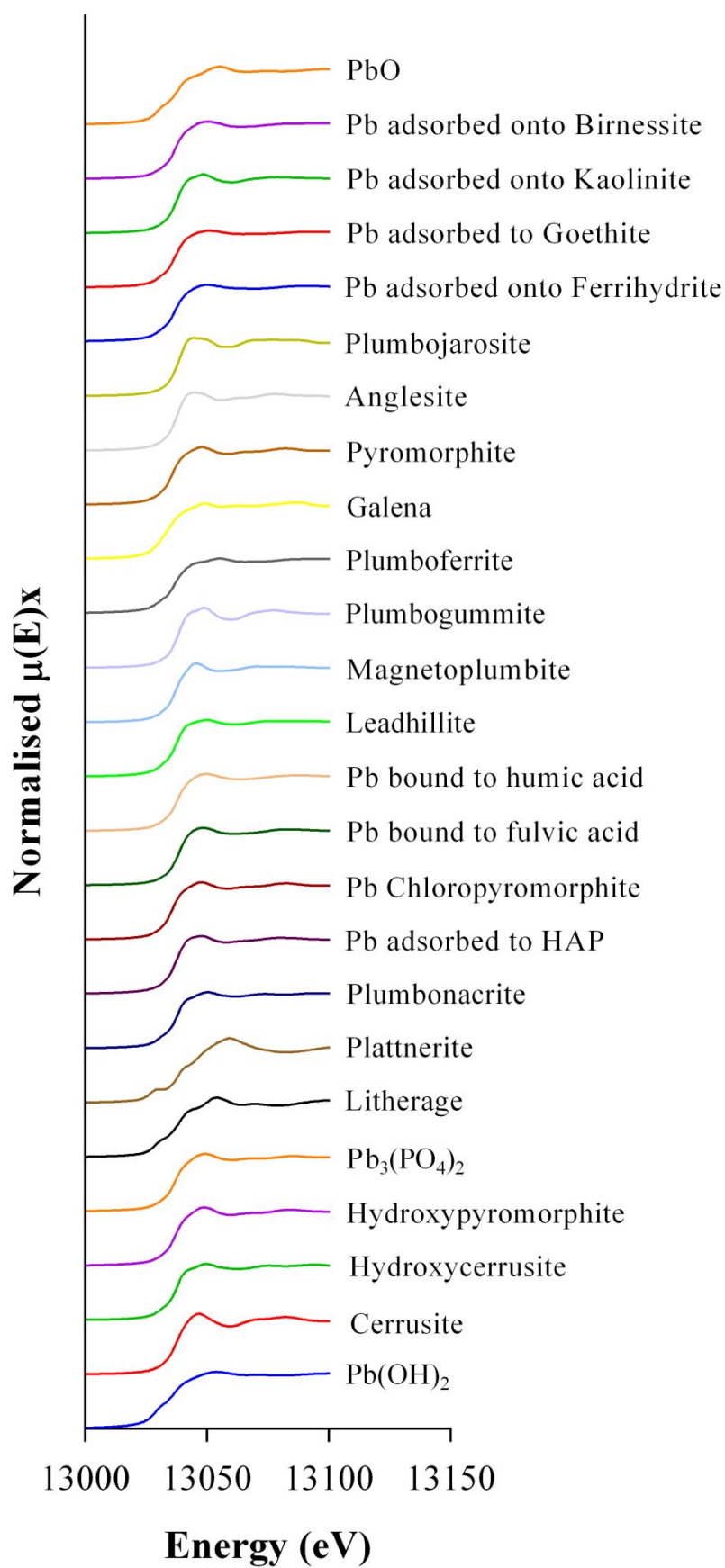
Figure S1: Standard spectra used for LCF fitting using XANES

Physico-chemical characteristics of soil

Table S1: Change in pH, Pb and P concentration before and after amending with phosphoric acid (PA), hydroxyapatite (HA), mono ammonium phosphate (MAP), triple super phosphate (TSP), bonemeal biochar and Fe_2O_3

		Type of amendment						
		Unamended	PA	HA	MAP	TSP	Biochar	Fe_2O_3
pH		5.8±0.07	3.7±0.02	5.4±0.14	5. 9±0.05	4.8±0.05	6.5±0.02	5.8±0.02
Ingestible fraction (<250 μm)								
Concentration (mg/kg)	Pb	14412±315	13233±123	13610±291	14345±468	13635±105	14034±416	13310±250
	P	637±13.2	6499±40.6	10693±275	5867±112	8390±157	7469±128	634±32.7
Molar ratio	P:Pb	0.3	3.3	5.3	2.7	4.1	3.6	0.3
Inhalable dust fraction (<10 μm)								
Broken-Hill	Pb (mg/kg)	65467±458	58519±970	44564±152	56431±1235	47982±126	46371±488	56200±199
	P (mg/kg)	1217±5.0	28739±392	62814±736	21218±431	26889±63.2	8638±141	1013±15.6
Molar ratio	P:Pb	0.1	3.3	9.4	2.5	3.7	1.2	0.1

Table S2: Fe speciation (Weighted %) in the < 10 μm particle size fraction. PA = phosphoric acid, HA = hydroxyapatite, TSP = triple super phosphate.

|	Ferrihydrite $(Fe(OH)_3)$	Goethite $(FeO(OH)$	Magnetite (Fe_3O_4)	Hematite $(\alpha\text{-}Fe_2O_3)$	Maghemite $(\gamma\text{-}Fe_2O_3)$	Clay	R-factor
No amendment	38	14	9	8	5	26	0.0011
PA	42	11	7	5	0	35	0.0012
HA	24	15	5	6	10	40	0.0022
TSP	42	8	8	15	2	26	0.002

Treatment efficacy

Table S3: Summary of treatment effect ratios (TER) for Pb amended soils. PA = phosphoric acid, HA = hydroxyapatite, MAP = monoammonium phosphate, TSP = triple super phosphate.

| Exposure pathway	Assay	Phase of assay	Amendment type					
			PA	HA	MAP	TSP	Biochar	Fe_2O_3
Ingestion	SBRC*	Gastric	1.03	1.02	1.05	1.08	1.03	1.06
		Intestinal	0.09	0.02	0.13	0.07	0.05	1.08
Inhalation	IIBA**	Lung	0.33	1.13	0.37	0.48	1.00	0.96
		Lung + intestinal	0.67	1.13	0.60	0.80	1.03	0.97

*Solubility Bioaccessibility Research Consortium assay

**Inhalation Ingestion Bioaccessibility Assay
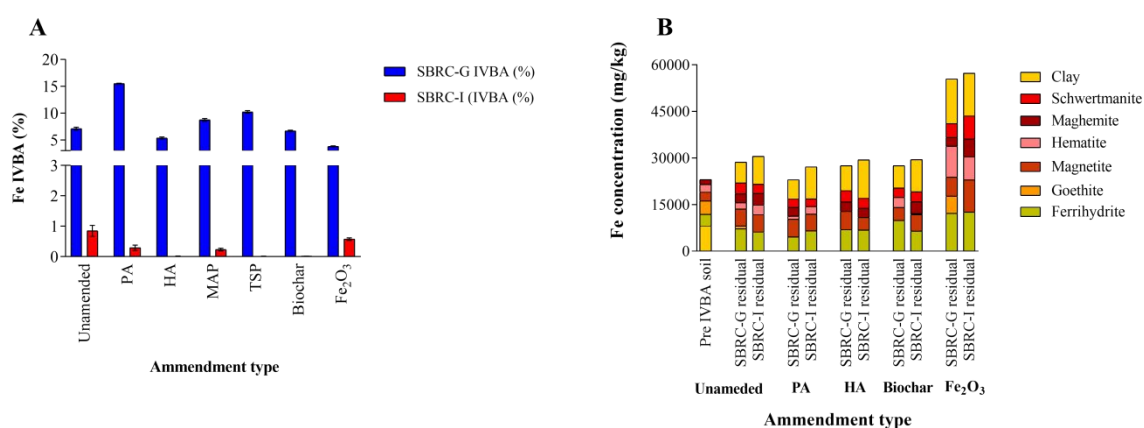
Figure S2: (A) Fe IVBA (%) using the Solubility Bioaccessibility Research Consortium (SBRC) assay where SBRC-G = extraction using the gastric phase and SBRC-I = extraction

using the gastro-intestinal (GI) phase. (B) change in Fe speciation (mg/kg) in the pre- and post-SRBC assay residuals. PA = phosphoric acid, HA = hydroxyapatite, MAP = monoammonium phosphate, TSP = triple super phosphate.
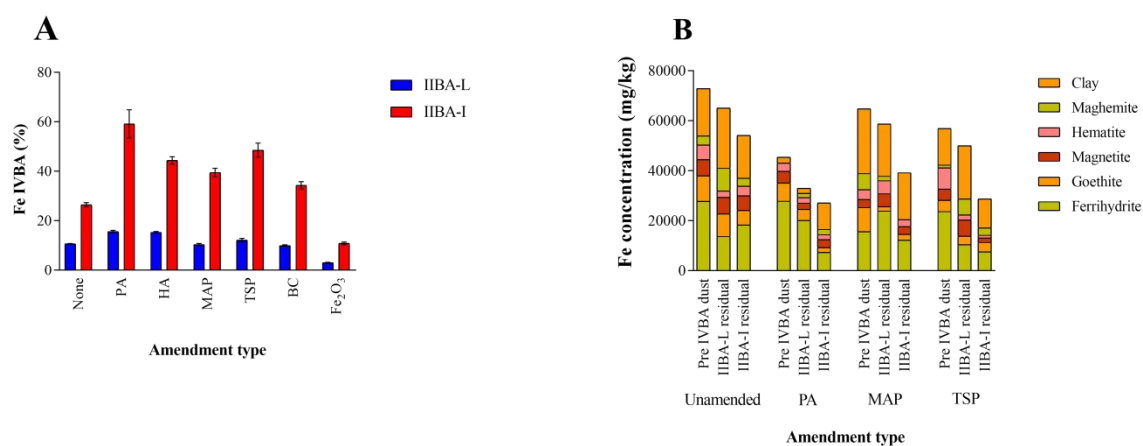
Figure S3: (A) Fe IVBA (%) using the Inhalation-Ingestion Bioaccessibility Assay (IIBA) where IIBA-L = extraction using the lung phase, IIBA-I = extraction using the lung+GI phase. (B) Fe speciation in pre- and post-IIBA assay residuals. PA = phosphoric acid, HA = hydroxyapatite, MAP = monoammonium phosphate, TSP = triple super phosphate, BC = biochar.
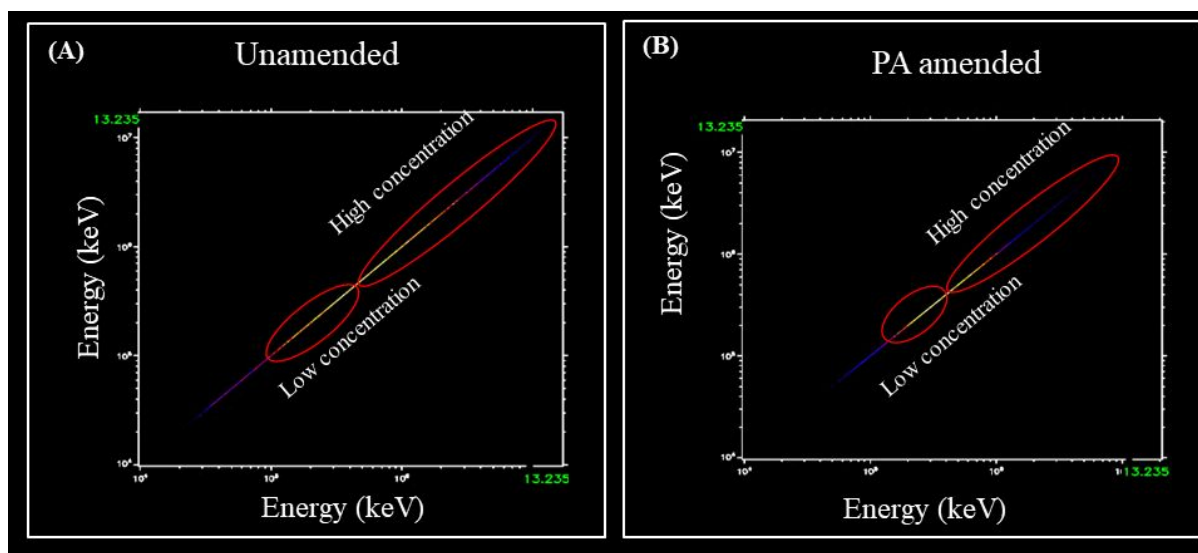
Figure S4: Regions of high and low Pb concentration used to obtain spectra for linear combination fitting (LCF) where (A) unamended and (B) amended samples. LCF fitting as conducted using references described in S.1 Spectroscopic assessment of phosphate amended Pb-contaminated soils.

References

(1)   EPA: Method 6020A (SW-846): Inductively Coupled Plasma-Mass Spectrometry, Revision 1. **1998**.

(2)   Klementiev, K.; Chernikov, R.: XAFSmass: a program for calculating the optimal mass of XAFS samples. *Journal of Physics: Conference Series* **2016**, *712*, 012008.

(3)   Ravel, B.; Newville, M.: ATHENA, ARTEMIS, HEPHAESTUS: data analysis for X-ray absorption spectroscopy using IFEFFIT. *J Synchrotron Radiat* **2005**, *12*, 537-41.

(4)   Webb, S. M.: SIXPack a Graphical User Interface for XAS Analysis Using IFEFFIT. *Physica Scripta* **2005**, 1011.

(5)   Paterson, D.; de Jonge, M. D.; Howard, D. L.; Lewis, W.; McKinlay, J.; Starritt, A.; Kusel, M.; Ryan, C. G.; Kirkham, R.; Moorhead, G.; Siddons, D. P.: The X-ray Fluorescence Microscopy Beamline at the Australian Synchrotron. *AIP Conference Proceedings* **2011**, *1365*, 219-222.

(6)   Paterson, D. J.; Boldeman, J. W.; Cohen, D. D.; Ryan, C. G.: Microspectroscopy Beamline at the Australian Synchrotron. *AIP Conference Proceedings* **2007**, *879*, 864-867.

(7)   Kirkham, R.; Dunn, P. A.; Kuczewski, A. J.; Siddons, D. P.; Dodanwela, R.; Moorhead, G. F.; Ryan, C. G.; De Geronimo, G.; Beuttenmuller, R.; Pinelli, D.; Pfeffer, M.; Davey, P.; Jensen, M.; Paterson, D. J.; de Jonge, M. D.; Howard, D. L.; Küsel, M.; McKinlay, J.: The Maia Spectroscopy Detector System: Engineering for Integrated Pulse Capture, Low-Latency Scanning and Real-Time Processing. *AIP Conference Proceedings* **2010**, *1234*, 240-243.

(8)   Ryan, C.: Quantitative trace element imaging using PIXE and the nuclear microprobe. *International Journal of Imaging Systems and Technology* **2000**, *11*, 219-230.

(9)   Ryan, C. G.; Jamieson, D. N.: Dynamic analysis: on-line quantitative PIXE microanalysis and its use in overlap-resolved elemental mapping. *Nuclear Instruments and Methods in Physics Research Section B: Beam Interactions with Materials and Atoms* **1993**, *77*, 203-214.